

# Joint analysis of Higgs decays and electroweak precision observables in the Standard Model with a sequential fourth generation

Otto Eberhardt<sup>a</sup>, Geoffrey Herbert<sup>b</sup>, Heiko Lacker<sup>b</sup>,  
Alexander Lenz<sup>c</sup>, Andreas Menzel<sup>b</sup>, Ulrich Nierste<sup>a</sup>, and Martin Wiebusch<sup>a</sup>

<sup>a</sup> *Institut für Theoretische Teilchenphysik, Karlsruhe Institute of Technology, D-76128 Karlsruhe, Germany, email: otto.eberhardt@kit.edu, ulrich.nierste@kit.edu, martin.wiebusch@kit.edu*

<sup>b</sup> *Humboldt-Universität zu Berlin, Institut für Physik, Newtonstr. 15, D-12489 Berlin, Germany, e-mail: geoffrey.herbert@physik.hu-berlin.de, lacker@physik.hu-berlin.de, amenzel@physik.hu-berlin.de*

<sup>c</sup> *CERN - Theory Division, PH-TH, Case C01600, CH-1211 Geneva 23, e-mail: alenz@cern.ch*

(Dated: August 28, 2012)

We analyse the impact of LHC and Tevatron Higgs data on the viability of the Standard Model with a sequential fourth generation (SM4), assuming Dirac neutrinos and a Higgs mass of 125 GeV. To this end we perform a combined fit to the signal cross sections of  $pp \rightarrow H \rightarrow \gamma\gamma, ZZ^*, WW^*$  at the LHC, to  $p\bar{p} \rightarrow VH \rightarrow Vb\bar{b}$  ( $V = W, Z$ ) at the Tevatron and to the electroweak precision observables. Fixing the mass of the fourth generation down-type quark  $b'$  to 600 GeV we find best-fit values of  $m_{t'}$  = 632 GeV,  $m_{t_4}$  = 113.6 GeV and  $m_{\nu_4}$  = 58.0 GeV for the other fourth-generation fermion masses. We compare the  $\chi^2$  values and pulls of the different observables in the three and four-generation case and show that the data is better described by the three-generation Standard Model. We also investigate the effects of mixing between the third and fourth-generation quarks and of a future increased lower bound on the fourth-generation charged lepton mass of 250 GeV.

## INTRODUCTION

While the Standard Model (SM) possesses a minimal boson field content, it indulges itself in the luxury of replicated fermion generations. It is difficult to predict the number of generations from fundamental theoretical principles; the determination of the correct number of fermion families is ultimately an experimental task. A sequential fourth generation is non-decoupling, meaning that its effect on certain observables does not vanish in the limit of infinitely heavy fourth-generation fermions. Among these observables are the gluon-fusion Higgs production cross section and the decay rate of  $H \rightarrow \gamma\gamma$ . This feature makes the SM with four generations, SM4, prone to be the first popular model of new physics on which the LHC will speak a final verdict.

Within the three generation SM (SM3) the production cross section  $\sigma(gg \rightarrow H)$ , which governs  $pp \rightarrow H$  studied at the LHC, is dominated by a triangle diagram with a top quark. While the loop diagram decreases as  $1/m_t$  for  $m_t \rightarrow \infty$ , this decrease is compensated by the linear growth of the top Yukawa coupling  $y_t \propto m_t$ . Consequently, in the SM4 the new contributions from the heavy  $t'$  and  $b'$  quarks will modify  $\sigma(gg \rightarrow H)$  by a term which is independent of  $m_{t'}$  and  $m_{b'}$  at the one-loop level. One finds an increase by roughly a factor of 9, which seemingly entails a corresponding increase in the LHC signal cross section of Higgs decays into (virtual) gauge bosons, given by the product  $\sigma(pp \rightarrow H)\mathcal{B}(H \rightarrow WW^*, ZZ^*, \gamma\gamma)$ . However, higher-order corrections to the Higgs production cross sections and branching ratios due to the fourth-generation fermions can be substantial because of their large Yukawa couplings. In [1–4] it was shown that, for

light Higgs bosons, the  $H \rightarrow WW^*$  and  $H \rightarrow ZZ^*$  branching ratios in the SM4 can be suppressed by a factor of 0.2 or less as compared to their SM3 values. In the photonic Higgs decay rate  $\Gamma(H \rightarrow \gamma\gamma)$  the destructive interference between fermion and gauge boson mediated contributions even leads to an accidental cancellation which would render the  $H \rightarrow \gamma\gamma$  decay unobservable. As pointed out in [5], this leads to tensions with the observed excesses in  $H \rightarrow \gamma\gamma$  searches at LHC and the searches for  $H \rightarrow b\bar{b}$  in  $HW, HZ$  associated production at the Tevatron.

In [6–13] it was discussed that the SM4 may permit the decay mode  $H \rightarrow \nu_4\bar{\nu}_4$ , where  $\nu_4$  denotes the neutrino of the fourth generation. If the  $\nu_4$  is sufficiently long-lived, LHC triggers will not associate the  $\nu_4$  decay with the primary Higgs production and decay event, such that  $H \rightarrow \nu_4\bar{\nu}_4$  will stay undetected. That is, with present experimental techniques the mere effect of an open  $H \rightarrow \nu_4\bar{\nu}_4$  channel will be an increase of the total Higgs width and thus a decrease of all other branching fractions. In this paper we will only consider the case of Dirac neutrinos. The fourth-generation neutrino must therefore be heavier than  $M_Z/2$  to comply with the invisible  $Z$  width measured at LEP1. While a nonzero  $H \rightarrow \nu_4\bar{\nu}_4$  decay rate can reconcile the LHC data on  $\sigma(pp \rightarrow H)\mathcal{B}(H \rightarrow WW^*, ZZ^*)$  with the SM4, it will only increase the tensions with the excesses in  $H \rightarrow \gamma\gamma$  at the LHC and  $H \rightarrow b\bar{b}$  at the Tevatron.

In [5] it was shown that the signals for  $H \rightarrow \gamma\gamma$  and  $H \rightarrow b\bar{b}$  can single-handedly rule out the SM4 if the currently measured signal cross sections are confirmed with significantly smaller errors. However, with the current uncertainties one must resort to a global fit to all rele-

vant observables to assess the viability of the SM4. The non-decoupling property of the SM4 implies that the SM3 can not be considered as a special case of the SM4 where some parameters are fixed. This actually represents a conceptual problem for a standard frequentist analysis as the choice of a suitable test statistic for the definition of  $p$ -values is no longer straightforward. We do not attempt to solve this issue here. Instead we simply compare the  $\chi^2$  values of the two models and the pulls of the individual observables. In all our fits we assume that the observed excesses in  $H \rightarrow \gamma\gamma$  and  $H \rightarrow b\bar{b}$  searches are not statistical fluctuations and we therefore fix the Higgs mass at  $m_H = 125$  GeV.

Stringent constraints on the SM4 are also found from analyses of the electroweak precision observables [14], because the extra fermions induce non-decoupling contributions to the  $W$  mass, partial  $Z$  decay widths and asymmetries which are very sensitive to the mass splittings within the fermionic isospin doublets. It has been shown in Ref. [15–20] that the SM4 is compatible with the experimental constraints from LEP if the  $m_{\nu'}-m_{b'}$  and/or  $m_{l_4}-m_{\nu_4}$  mass splittings are chosen properly. Here  $l_4$  denotes the charged lepton of the fourth generation. In this letter we perform a global fit to the parameters of the SM4, using the LHC data on the abovementioned Higgs decays, Tevatron data on  $H \rightarrow b\bar{b}$  and electroweak precision data. We also discuss the impact of mixing between the third and fourth-generation quarks as well as the impact of an increased lower bound on the fourth generation charged lepton mass. For our fits we use the CKMfitter package, which implements the Rfit procedure [21], a frequentist statistical method.

## METHODOLOGY

The main topic of this letter is a combined fit of the following (pseudo-)observables, which defines our analysis A1:

- i) the signal strengths  $\hat{\mu}(pp \rightarrow H \rightarrow WW^*)$  measured by CMS [22] (defined below) and  $\hat{\mu}(pp \rightarrow H \rightarrow ZZ^*)$  measured by CMS [22] and ATLAS [23],
- ii) the signal strengths  $\hat{\mu}(VV \rightarrow H \rightarrow \gamma\gamma)$  and  $\hat{\mu}(gg \rightarrow H \rightarrow \gamma\gamma)$  for Higgs production via vector boson fusion and gluon fusion, respectively, and subsequent decay into two photons as measured by CMS [24] and ATLAS [25],
- iii) the signal strength  $\hat{\mu}(p\bar{p} \rightarrow HV \rightarrow Vb\bar{b})$  for Higgs production in association with a vector boson and subsequent decay into a  $b\bar{b}$  pair, as measured by CDF and D0 [26],
- iv) the electroweak precision observables (EWPOs)  $M_Z, \Gamma_Z, \sigma_{\text{had}}, A_{\text{FB}}^l, A_{\text{FB}}^c, A_{\text{FB}}^b, A_l, A_c, A_b, R_l =$

$\Gamma_{l+l-}/\Gamma_{\text{had}}, R_c, R_b, \sin^2\theta_l^{\text{eff}}$  measured at LEP and SLC [27] as well as  $m_t, M_W, \Gamma_W$  and  $\Delta\alpha_{\text{had}}^{(5)}$  [14].

- v) the lower bounds  $m_{t',b'} \gtrsim 600$  GeV (from the LHC) [28–31] and  $m_{l_4} > 101$  GeV (from LEP2) [14].

Here and in the following, the term “signal strength” refers to the ratio of SM4 and SM3 signal cross sections evaluated with the same Higgs mass

$$\hat{\mu}(X \rightarrow H \rightarrow Y) = \frac{\sigma(X \rightarrow H)\mathcal{B}(H \rightarrow Y)|_{\text{SM4}}}{\sigma(X \rightarrow H)\mathcal{B}(H \rightarrow Y)|_{\text{SM3}}} \quad (1)$$

where a signal cross section is given by the product of the Higgs production cross section and a branching fraction into a certain final state.

When confronting the SM4 with electroweak precision data, the usual method is to compute the oblique electroweak parameters  $S$  and  $T$  [32], and compare the results to the best-fit values for  $S$  and  $T$  provided by the LEP Electroweak Working Group [27]. For the SM4, such studies were done, for example, in Refs. [14, 19, 20, 33]. However, it is well-known that the parametrisation of the EWPOs (iv) by  $S$  and  $T$  becomes inaccurate when some of the fourth-generation fermion masses are close to  $M_Z$  or when the fourth-generation fermions mix with the fermions of the first three generations. Since here, we are interested in a scenario where  $m_{\nu_4} < M_Z$  we do not use the oblique electroweak parameters in our analysis, but fit the EWPOs directly. To this end, we use ZFitter [34–36] to compute accurate predictions for the EWPOs in the SM3. (More precisely, we use the DIZET subroutine of the ZFitter package.) Then we follow the procedure of [37] and add corrections due to the fourth-generation fermions to the EWPOs. The differences between EWPOs in the SM4 and SM3 are calculated at one-loop order, but no further approximations are made for the EWPOs. As experimental inputs we use  $M_W = 80.390 \pm 0.016$  GeV [38] and otherwise the same inputs as the GFitter collaboration [39]. With our program we reproduce the best-fit parameters and observables for the SM3 within less than 10% of the (fit) error quoted in [39] for each parameter or observable. Our electroweak fit differs from the one in [39] in two points: we neglect the bottom and charm mass in the calculation of the EWPOs and we do not include theoretical errors. For the present analysis we also fix the Higgs mass to 125 GeV.

The current limit on the  $b'$  mass according to [30] is approximately 600 GeV. However, this and other limits on fourth generation quark masses by CMS and ATLAS rely on certain assumptions about the decay pattern of the quarks. These limits can be severely weakened if CKM mixing and ‘cascade decays’ such as  $t' \rightarrow b'W$  are taken into account [40]. In this letter we avoid the bounds on fourth-generation quark masses by fixing the  $b'$  mass to  $m_{b'} = 600$  GeV. The splitting between the fourth-generation quark masses is strongly constrained by the

EWPOs, so that the bound on  $m_{t'}$  will automatically be satisfied.

In close correspondence to SM3 electroweak fits such as [14, 39], we let the following parameters float in our fit:

$$\Delta\alpha_{\text{had}}^{(5)}, \alpha_s, M_Z, m_t, m_{t'}, m_{\nu_4}, m_{l_4} \text{ and } \theta_{34}, \quad (2)$$

where  $\Delta\alpha_{\text{had}}^{(5)}$  is the hadronic contribution to the running of the fine-structure constant in the 5-flavour scheme and  $\theta_{34}$  denotes the mixing angle between the third and fourth generation, defined analogously to the Cabibbo angle. The importance of the mixing angle  $\theta_{34}$  in the SM4 electroweak fit was pointed out in [41]. Mixing of the fourth generation with the first two generations and additional  $CP$  violating phases can be relevant if flavour observables are included in the fit. However, the constraints on these parameters from flavour physics are so strong that the allowed variations do not have a big effect on the observables studied in this letter. We therefore set these additional phases and mixing angles to zero. Note that we fix the Higgs mass to 125 GeV, which is the value favoured by the hints seen in 2011 LHC data. The choice of a fixed value for  $m_{b'}$  does not lead to a significant loss of generality, as the experimental lower bound  $m_{b'} \gtrsim 600$  GeV [30] is already rather close to the scale where the Yukawa interactions become non-perturbative [42]. Also, the non-decoupling property of the most relevant quantities implies a rather mild dependence on  $m_{b'}$ .

We include the two-loop electroweak corrections to Higgs production and decay in our evaluation of the Higgs signal cross sections in the SM4 by means of the program HDECAY v. 4.45 [43]. This is mandatory, because the flat dependence of these decay amplitudes on  $m_{t',b',l_4}$  is broken by the leading two-loop corrections [4]. To avoid the complicated procedure of interfacing the HDECAY code with our program we set — for the evaluation of the Higgs signal cross sections —  $m_{t'} = 650$  GeV,  $\theta_{34} = 0$  and the SM parameters  $\alpha$ ,  $\alpha_s$ ,  $M_Z$  and  $m_t$  to the default values of HDECAY. The dependence of the cross sections on  $m_{\nu_4}$  and  $m_{l_4}$  is then accounted for by linear interpolation of two-dimensional lookup-tables with a granularity of 0.5 GeV for  $m_{\nu_4}$  and 50 GeV for  $m_{l_4}$ . As the experimental errors on the Higgs signal cross sections are still rather large this simplification has no noticeable impact on our fit.

Table I summarises our experimental inputs for the Higgs signal strengths in the different search channels: The signal strength for Higgs production via vector boson fusion (VBF) and subsequent decay into  $\gamma\gamma$  ( $VV \rightarrow H \rightarrow \gamma\gamma$ ) corresponds to the signal strength for the dijet class in [24]. We assume that the events in this category stem entirely from vector boson fusion processes. This is, of course, a somewhat crude approximation. There will also be a certain contamination from gluon fusion events in that sample, but lacking more detailed information on

process	signal strength	reference
$VV \rightarrow H \rightarrow \gamma\gamma$	$3.7_{-1.7}^{+2.0}$	[24]
$gg \rightarrow H \rightarrow \gamma\gamma$	$1.30_{-0.50}^{+0.49}$	[24, 25]
$pp \rightarrow H \rightarrow WW^*$	$0.39_{-0.56}^{+0.61}$	[22]
$pp \rightarrow H \rightarrow ZZ^*$	$0.69_{-0.52}^{+0.93}$	[22, 23]
$p\bar{p} \rightarrow HV \rightarrow Vb\bar{b}$	$2.03_{-0.71}^{+0.73}$	[26]

TABLE I. Experimental inputs for Higgs signal strengths at  $m_H = 125$  GeV.

this contamination we are forced to ignore it. The signal strength for Higgs production via gluon fusion and subsequent decay into  $\gamma\gamma$  ( $gg \rightarrow H \rightarrow \gamma\gamma$ ) was obtained by removing the dijet contribution from the combined result for the signal strength in [24] and combining the result with the one from [25]. In doing this, we implicitly neglect all Higgs production mechanisms except gluon fusion and vector boson fusion. The signal strength for  $pp \rightarrow H \rightarrow ZZ^*$  is a combination of the results presented in [22] and [23]. The signal strength for  $pp \rightarrow H \rightarrow WW^*$  was taken from [22]. The input for the  $p\bar{p} \rightarrow HV \rightarrow Vb\bar{b}$  process is taken from the latest Tevatron search [26] for Higgs bosons produced in association with a  $W$  or  $Z$  boson and subsequently decaying into a  $b\bar{b}$  pair.

For the computation of signal cross sections in the SM4 we use an effective coupling approximation along the lines of [44, 45]. Specifically, we calculate the SM4 signal cross sections by taking SM3 production cross sections for the different production mechanisms from [46] (LHC) and [47, 48] (Tevatron), scaling them with corresponding SM4/SM3 ratios of related partial Higgs decay widths and multiplying with the SM4 branching fractions calculated by HDECAY. For instance, the SM4 signal cross section for  $gg \rightarrow H \rightarrow \gamma\gamma$  is calculated as

$$\sigma(gg \rightarrow H \rightarrow \gamma\gamma)_{\text{SM4}} = \sigma(gg \rightarrow H)_{\text{SM3}} \times \frac{\Gamma(H \rightarrow gg)_{\text{SM4}}}{\Gamma(H \rightarrow gg)_{\text{SM3}}} \mathcal{B}(H \rightarrow \gamma\gamma)_{\text{SM4}}, \quad (3)$$

with  $\sigma(gg \rightarrow H)_{\text{SM3}}$  taken from [46] and the remaining quantities on the right-hand side calculated by HDECAY. The factor  $\Gamma(H \rightarrow gg)_{\text{SM4}}/\Gamma(H \rightarrow gg)_{\text{SM3}}$  accounts for the modified  $Hgg$  effective coupling in the SM4. For the VBF process  $VV \rightarrow H \rightarrow \gamma\gamma$  the Higgs can come from a  $HWW$  or  $HZZ$  vertex. We assume that 75% of the production cross section comes from  $WW$  fusion and 25% from  $ZZ$  fusion. These ratios were obtained from [49], which implements the NLO results from [50]. Equations analogous to (3) are then used separately for the  $WW \rightarrow H$  and  $ZZ \rightarrow H$  production modes. For the  $pp \rightarrow H \rightarrow WW^*$  and  $pp \rightarrow H \rightarrow ZZ^*$  signal cross sections all production mechanisms were taken into account. For the (Tevatron)  $p\bar{p} \rightarrow HV \rightarrow Vb\bar{b}$  process only the  $HW$  and  $HZ$  associated production mechanisms

contribute. The corresponding SM3 production cross sections were taken from [48]. Like the LHC cross sections these were scaled with the SM4/SM3 ratios of  $H \rightarrow WW$  and  $H \rightarrow ZZ$  partial widths, respectively, and multiplied with the SM4  $H \rightarrow b\bar{b}$  branching fraction.

In order to disentangle the impacts of the Higgs searches and the electroweak precision observables we perform a second fit, denoted as analysis A2. In this analysis we only fit the Higgs data, ignoring the EWPOs altogether. Here we only let  $m_{\nu_4}$  and  $m_{l_4}$  float, while keeping  $m_{t'}$  fixed to 650 GeV.

## RESULTS

From Table I we see that the searches for  $VV \rightarrow H \rightarrow \gamma\gamma$  and  $p\bar{p} \rightarrow HV \rightarrow Vb\bar{b}$  prefer an enhancement of the SM signal while the searches for  $pp \rightarrow H \rightarrow WW^*$  and  $pp \rightarrow H \rightarrow ZZ^*$  prefer reduced signals. Thus, only the  $pp \rightarrow H \rightarrow WW^*$  and  $pp \rightarrow H \rightarrow ZZ^*$  searches favour a large invisible Higgs decay width and our fits must choose a neutrino mass that compromises between the two tendencies. The result of our analysis A2 (fitting Higgs signal strengths only) is  $m_{\nu_4} = 60$  GeV and  $m_{l_4} = 600$  GeV (the latter being the upper end of the range in which  $m_{l_4}$  was allowed to float). So, the best-fit neutrino mass is just below the  $H \rightarrow \nu_4\bar{\nu}_4$  threshold, leading to  $\mathcal{B}(H \rightarrow \nu_4\bar{\nu}_4) \approx 0.46$ . The minimum  $\chi^2$  value in this fit is 18.2. This should be compared to the  $\chi^2$  value of 6.1, which is obtained in the SM3. These results agree with a recent analysis of this type by Kuflik, Nir and Volansky [51]. Their conversion of the  $\chi^2$  values to confidence levels should however be taken with a grain of salt since, in their analysis, some of the SM4 parameters were scanned over but not counted as degrees of freedom when converting  $\chi^2$  values into confidence levels. In general, the number of degrees of freedom of a fit is ill-defined when parameters are only allowed to float within a certain range (such as the fourth generation fermion masses) and the relation between the  $\chi^2$  value and the confidence level is no longer described by the normalised lower incomplete gamma function. Due to the afore-mentioned conceptual problems with the definition of a suitable test statistic for the comparison of SM4 and SM3 we refrain from converting our  $\chi^2$  values into  $p$ -values and only discuss the pulls of the individual signal strengths. We hope to shed more light on the issue of a quantitative comparison of the SM3 and SM4 in a future publication.

The best-fit charged lepton mass in the analysis A2 is at the upper end of the range in which it was allowed to float. Of course, such a large mass splitting within the lepton doublet is ruled out by electroweak precision data. In our analysis A1 (combination of EWPOs and Higgs signal strengths) we obtain the following best-fit

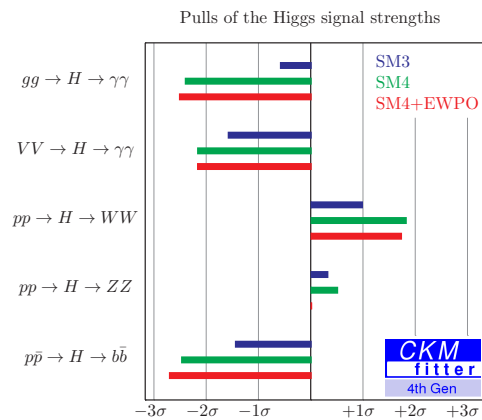


FIG. 1. Deviations (pulls) of the predicted signal strengths from the measured signal strengths in units of the experimental errors. The pulls are shown for the SM3 and the two SM4 scenarios, corresponding to our analyses A1 (SM4 w. EWPO) and A2 (SM4 w/o EWPO).

values:

$$\begin{aligned} m_{\nu_4} &= 58.0 \text{ GeV} , & m_{l_4} &= 113.6 \text{ GeV} , \\ m_{t'} &= 632 \text{ GeV} , & \chi_{\text{SM4},\text{min}}^2 &= 33.4 . \end{aligned} \quad (4)$$

We see that the best-fit charged lepton mass is now just above the LEP limit. The best-fit neutrino mass has moved to a slightly lower value, leading to  $\mathcal{B}(H \rightarrow \nu_4\bar{\nu}_4) \approx 0.66$ . The minimum  $\chi^2$  value should be compared with the SM3 value  $\chi_{\text{SM3},\text{min}}^2 = 21.7$ .

Figure 1 shows the pulls of the signal strengths in the SM3 and SM4 for our analyses A1 and A2. The pulls are defined as  $(\hat{\mu}_{\text{pred}} - \hat{\mu}_{\text{exp}})/\Delta\hat{\mu}$ , where  $\hat{\mu}_{\text{exp}}$  and  $\Delta\hat{\mu}$  are the experimental values and errors of the signal strengths in Table I and  $\hat{\mu}_{\text{pred}}$  is obtained by removing the experimental input for the corresponding signal strength from the fit and using the other observables to predict its value. We see that the pulls for the analyses A1 and A2 are essentially the same. This can be understood as follows: the main effect of including the EWPOs in the fit is that the lepton mass is constrained to smaller values, but the Higgs signal strengths are not sensitive enough to the lepton mass for this to make a big difference. With the exception of  $pp \rightarrow H \rightarrow ZZ^*$ , the pulls in the SM4 are always bigger than in the SM3, their magnitude being around  $2\sigma$ . For  $pp \rightarrow H \rightarrow ZZ^*$  the predicted SM4 signal strength is equal to the measured one while the pull in the SM3 is about  $0.5\sigma$ . This agreement of the SM4 is however purely accidental.

In Fig. 2 we show the minimum  $\chi^2$  as a function of  $m_{\nu_4}$  and minimised with respect to the other parameters in (2) for our analyses A1 and A2. The  $\chi^2$  value of the SM3 is indicated by the dotted line. We see that the SM3 has a smaller  $\chi^2$  value than the SM4 for any choice of  $m_{\nu_4}$ . In both analyses the best-fit value of  $m_{\nu_4}$  is near 60 GeV, i.e. just below the  $H \rightarrow \nu_4\bar{\nu}_4$  threshold.

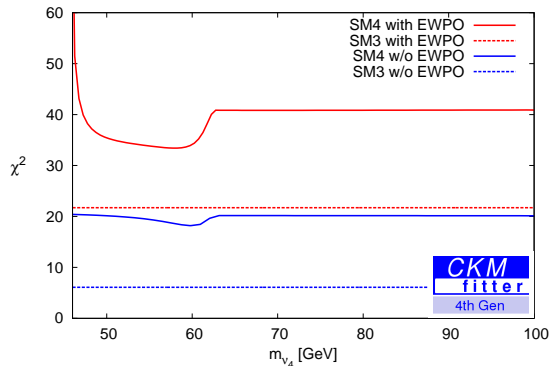


FIG. 2. Minimum  $\chi^2$  values for a fixed neutrino mass as a function of  $m_{\nu_4}$ . Results are shown for the two SM4 analyses A1 (red) and A2 (blue). The dotted lines indicate the corresponding SM3 minimal  $\chi^2$  value.

For  $m_{\nu_4} \lesssim 60$  GeV the Higgs signal strengths favour a small lepton mass while for  $m_{\nu_4} \gtrsim 60$  GeV a large charged lepton mass is preferred by direct Higgs searches. Since EWPOs forbid too large mass splittings (of order 100 GeV or more) in the lepton doublet the increase of  $\chi^2$  at  $m_{\nu_4} \approx 60$  GeV is more pronounced in the analysis A1. Above the  $H \rightarrow \nu_4 \bar{\nu}_4$  threshold the  $\chi^2$  value is essentially independent of  $m_{\nu_4}$ . As  $m_{\nu_4}$  approaches  $M_Z/2$  the  $\chi^2$  in the analysis A1 blows up due to threshold effects in the EWPOs.

In a sensitivity study [52] for fourth-generation charged lepton searches at the LHC it was found that with  $1 \text{ fb}^{-1}$  of data the LHC experiments should be able to rule out a fourth-generation charged lepton with a mass below approximately 250 GeV. Currently there are no experimental results available for these searches. Let us nonetheless investigate what happens if the mass bound for the fourth-generation charge lepton moves up to 250 GeV. Fig. 3 shows the  $\chi^2$  of our analysis A1 with a modified charged lepton mass limit  $m_{l_4} > 250$  GeV as a function of  $m_{\nu_4}$ , minimized with respect to all other parameters. We see that the  $\chi^2$  is constant at a value of 36 for  $m_{\nu_4} \gtrsim 160$  GeV. For neutrino masses below 160 GeV the electroweak fit can no longer accommodate the large mass splitting in the lepton sector and the  $\chi^2$  blows up. Thus, for  $m_{l_4} > 250$  GeV (and the case of Dirac neutrinos) the scenario with the invisible  $H \rightarrow \nu_4 \bar{\nu}_4$  decay is completely ruled out by electroweak precision observables.

The impact of mixing between the third and fourth generation quark is negligible in the analysis A1. The fit prefers  $\theta_{34} = 0$  and therefore cannot be improved by letting  $\theta_{34}$  float. The constraint on  $\theta_{34}$  imposed by EWPOs and Higgs signal strengths can be studied by using the difference between the minimal  $\chi^2$  in the SM4 with  $\theta_{34}$  free and  $\theta_{34}$  fixed as a test statistic. Since we are now comparing two different realisations of the same model (SM4) there is no problem with the conversion of  $\chi^2$  values to  $p$ -values. Fig. 4 shows the  $p$ -value as a function  $\theta_{34}$ .

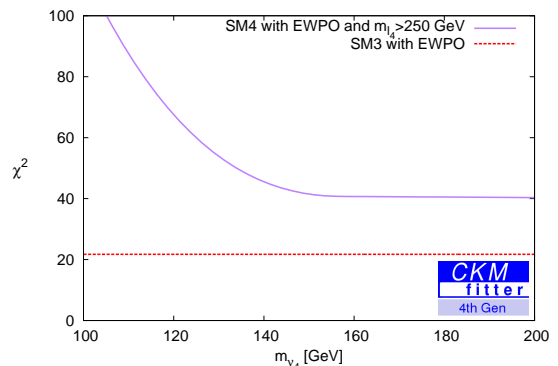


FIG. 3. Minimum  $\chi^2$  values in the analysis A1 for  $m_{l_4} > 250$  GeV as a function of the (fixed) neutrino mass  $m_{\nu_4}$ . The dotted lines indicate the corresponding SM3 minimal  $\chi^2$  value.

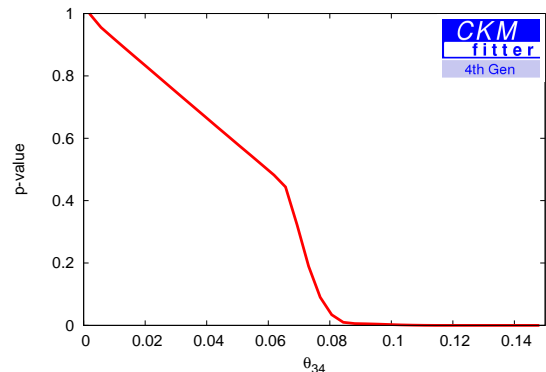


FIG. 4.  $p$ -value scan of the CKM mixing angle  $\theta_{34}$  between the third and fourth generation quarks in the analysis A1.

We see that Higgs signal strengths and EWPOs require  $\theta_{34} \lesssim 0.08$ . However, this picture could change dramatically if flavour observables were included in the fit: A recent analysis shows that the SM3 fails to describe flavour physics observables at the level of  $2.7\sigma$  [53–56]. Since the SM4 can alleviate the discrepancies in the flavour data, the overall picture may still change in favour of the SM4 in a complete analysis of Higgs decay, electroweak precision, and flavour data. Such an analysis is beyond the scope of this letter.

## CONCLUSIONS

Assuming a Higgs mass of 125 GeV we have performed a global fit to the parameters of the SM4, combining data on electroweak precision physics and five different Higgs searches:  $H \rightarrow \gamma\gamma$  produced by gluon fusion at the LHC,  $H \rightarrow \gamma\gamma$  produced by vector boson fusion at the LHC, inclusive searches for  $H \rightarrow WW, ZZ$  at the LHC and  $W, Z$  associated production and decay to  $b\bar{b}$  at the Tevatron. With the exception of the inclusive  $H \rightarrow ZZ$  search the pulls of the signal cross sections in

the SM4 exceed those of the SM3 by  $0.5\sigma$  or more. Also the electroweak precision observables are described better in the SM3. With a lower bound of 100 GeV on the fourth-generation charged lepton mass the best-fit SM4 scenario has a fourth-generation neutrino mass around 60 GeV, i.e. just below the  $H \rightarrow \nu_4 \bar{\nu}_4$  threshold. If the lower bound on the fourth-generation charged lepton mass moves up to 250 GeV the electroweak precision observables constrain  $m_{\nu_4}$  to be larger than approximately 160 GeV and scenarios with invisible  $H \rightarrow \nu_4 \bar{\nu}_4$  decays are ruled out. The mixing angle  $\theta_{34}$  between the third and fourth generation quarks is constrained to be smaller than 0.08. However, since the SM4 can alleviate the discrepancies in flavour observables, the overall picture may still change in favour of the SM4 when flavour observables are included in the fit. On the basis of electroweak precision data and Higgs searches alone the SM4 is certainly disfavoured. A quantitative comparison of the SM3 and SM4 in terms of  $p$ -values is problematic since classical likelihood ratio tests for nested models are inapplicable due to the non-decoupling nature of the SM4 fermions. We hope to shed more light on this subject in a future publication.

We would like to thank the CKMfitter group, in particular Jérôme Charles and Stéphane T’Jampens, for valuable input on statistical methods and CKMfitter software support. Further, we would like to thank Julien Baglio for fruitful discussions and help with the VBF cross sections. We acknowledge support by DFG through grants NI1105/2-1 and LA 2541/1-1. A.L. is further supported by DFG through a Heisenberg fellowship.

- 
- [1] A. Djouadi and P. Gambino, Phys.Rev. **D51**, 218 (1995), arXiv:hep-ph/9406431 [hep-ph]
- [2] A. Djouadi and P. Gambino, Phys.Rev.Lett. **73**, 2528 (1994), arXiv:hep-ph/9406432 [hep-ph]
- [3] G. Passarino, C. Sturm, and S. Uccirati, Phys.Lett. **B706**, 195 (2011), arXiv:1108.2025 [hep-ph]
- [4] A. Denner, S. Dittmaier, A. Muck, G. Passarino, M. Spira, *et al.*(2011), arXiv:1111.6395 [hep-ph]
- [5] A. Djouadi and A. Lenz(2012), arXiv:1204.1252 [hep-ph]
- [6] V. A. Khoze(2001), arXiv:hep-ph/0105069 [hep-ph]
- [7] K. Belotsky, D. Fargion, M. Khlopov, R. Konoplich, and K. Shibaev, Phys.Rev. **D68**, 054027 (2003), arXiv:hep-ph/0210153 [hep-ph]
- [8] S. Bulanov, V. Novikov, L. Okun, A. N. Rozanov, and M. Vysotsky, Phys.Atom.Nucl. **66**, 2169 (2003), arXiv:hep-ph/0301268 [hep-ph]
- [9] A. Rozanov and M. Vysotsky, Phys.Lett. **B700**, 313 (2011), arXiv:1012.1483 [hep-ph]
- [10] W.-Y. Keung and P. Schwaller, JHEP **1106**, 054 (2011), arXiv:1103.3765 [hep-ph]
- [11] S. Cetin, T. Cuhadar-Donszelmann, M. Sahin, S. Sultansoy, and G. Unel, Phys.Lett. **B710**, 328 (2012), arXiv:1108.4071 [hep-ph]
- [12] C. Englert, J. Jaeckel, E. Re, and M. Spannowsky, Phys.Rev. **D85**, 035008 (2012), arXiv:1111.1719 [hep-ph]
- [13] L. M. Carpenter(2011), arXiv:1110.4895 [hep-ph]
- [14] K. Nakamura *et al.* (Particle Data Group), J.Phys.G **G37**, 075021 (2010)
- [15] H.-J. He, N. Polonsky, and S.-f. Su, Phys.Rev. **D64**, 053004 (2001), arXiv:hep-ph/0102144 [hep-ph]
- [16] V. Novikov, L. Okun, A. N. Rozanov, and M. Vysotsky, JETP Lett. **76**, 127 (2002), arXiv:hep-ph/0203132 [hep-ph]
- [17] J.-M. Frere, A. Rozanov, and M. Vysotsky, Phys.Atom.Nucl. **69**, 355 (2006), arXiv:hep-ph/0412080 [hep-ph]
- [18] V. Novikov, A. Rozanov, and M. Vysotsky, Phys.Atom.Nucl. **73**, 636 (2010), dedicated to L.B. Okun’s 80th birthday, arXiv:0904.4570 [hep-ph]
- [19] G. D. Kribs, T. Plehn, M. Spannowsky, and T. M. Tait, Phys.Rev. **D76**, 075016 (2007), arXiv:0706.3718 [hep-ph]
- [20] O. Eberhardt, A. Lenz, and J. Rohrwild, Phys.Rev. **D82**, 095006 (2010), arXiv:1005.3505 [hep-ph]
- [21] A. Hocker, H. Lacker, S. Laplace, and F. Le Diberder, Eur.Phys.J. **C21**, 225 (2001), arXiv:hep-ph/0104062 [hep-ph]
- [22] CMS physics analysis summary, CMS PAS HIG-12-008, <https://cdsweb.cern.ch/record/1429928>
- [23] G. Aad *et al.* (ATLAS Collaboration), Phys. Lett. **B710**, 383 (2012), arXiv:1202.1415 [hep-ex]
- [24] CMS physics analysis summary, CMS PAS HIG-12-001, <http://cdsweb.cern.ch/record/1335713>
- [25] G. Aad *et al.* (ATLAS Collaboration), Phys.Rev.Lett. **108**, 111803 (2012), supplementary material at <https://atlas.web.cern.ch/Atlas/GROUPS/PHYSICS/PAPERS/HIGG-2012-02/>, arXiv:1202.1414 [hep-ex]
- [26] W. Fisher (CDF and D0), Talk given at Moriond 2012, <http://indico.in2p3.fr/getFile.py/access?contribId=87&sessionId=1&resId=0&materialId=slides&confId=6001>
- [27] ALEPH, CDF, D0, DELPHI, L3, OPAL, SLD, LEP Electroweak Working Group, Tevatron Electroweak Working Group, and SLD electroweak heavy flavour groups(2010), arXiv:1012.2367 [hep-ex]
- [28] G. Aad *et al.* (ATLAS Collaboration)(2012), arXiv:1202.3076 [hep-ex]
- [29] G. Aad *et al.* (ATLAS Collaboration)(2012), arXiv:1202.6540 [hep-ex]
- [30] C. Collaboration *et al.* (CMS Collaboration)(2012), arXiv:1204.1088 [hep-ex]
- [31] CMS physics analysis summary, CMS PAS EXO-11-099, <http://cdsweb.cern.ch/record/1428894>
- [32] M. E. Peskin and T. Takeuchi, Phys. Rev. **D46**, 381 (1992)
- [33] J. Erler and P. Langacker, Phys.Rev.Lett. **105**, 031801 (2010), arXiv:1003.3211 [hep-ph]
- [34] D. Y. Bardin, M. S. Bilenky, T. Riemann, M. Sachwitz, and H. Vogt, Comput.Phys.Commun. **59**, 303 (1990)
- [35] D. Y. Bardin, P. Christova, M. Jack, L. Kalinovskaya, A. Olchevski, *et al.*, Comput.Phys.Commun. **133**, 229 (2001), arXiv:hep-ph/9908433 [hep-ph]
- [36] A. Arbuzov, M. Awramik, M. Czakon, A. Freitas, M. Grunewald, *et al.*, Comput.Phys.Commun. **174**, 728 (2006), arXiv:hep-ph/0507146 [hep-ph]
- [37] P. Gonzalez, J. Rohrwild, and M. Wiebusch(2011), arXiv:1105.3434 [hep-ph]
- [38] T. Aaltonen *et al.* (CDF Collaboration)(2012), arXiv:1203.0275 [hep-ex]

- [39] M. Baak, M. Goebel, J. Haller, A. Hoecker, D. Ludwig, *et al.*(2011), arXiv:1107.0975 [hep-ph]
- [40] C. J. Flacco, D. Whiteson, T. M. Tait, and S. Bar-Shalom, Phys.Rev.Lett. **105**, 111801 (2010), arXiv:1005.1077 [hep-ph]
- [41] M. S. Chanowitz, Phys.Rev. **D79**, 113008 (2009), arXiv:0904.3570 [hep-ph]
- [42] M. S. Chanowitz, M. Furman, and I. Hinchliffe, Phys.Lett. **B78**, 285 (1978)
- [43] A. Djouadi, J. Kalinowski, and M. Spira, Comput.Phys.Commun. **108**, 56 (1998), sM4 contributions implemented since version 4.45, arXiv:hep-ph/9704448 [hep-ph]
- [44] P. Bechtle, O. Brein, S. Heinemeyer, G. Weiglein, and K. E. Williams, Comput.Phys.Commun. **181**, 138 (2010), arXiv:0811.4169 [hep-ph]
- [45] P. Bechtle, O. Brein, S. Heinemeyer, G. Weiglein, and K. E. Williams, Comput.Phys.Commun. **182**, 2605 (2011), arXiv:1102.1898 [hep-ph]
- [46] S. Dittmaier *et al.* (LHC Higgs Cross Section Working Group)(2011), updated results at <https://twiki.cern.ch/twiki/bin/view/LHCPhysics/CERNYellowReportPageAt7TeV>, arXiv:1101.0593 [hep-ph]
- [47] O. Brein, A. Djouadi, and R. Harlander, Phys.Lett. **B579**, 149 (2004), 13 pages, latex+axodraw, 8 figures (3 psfiles) Report-no: CERN TH/2003-161, MPP-2003-35, PM/03-16, arXiv:hep-ph/0307206 [hep-ph]
- [48] J. Baglio and A. Djouadi, JHEP **1010**, 064 (2010), arXiv:1003.4266 [hep-ph]
- [49] M. Spira, VV2H code, <http://people.web.psi.ch/spira/vv2h/>
- [50] T. Han, G. Valencia, and S. Willenbrock, Phys.Rev.Lett. **69**, 3274 (1992), arXiv:hep-ph/9206246 [hep-ph]
- [51] E. Kuffik, Y. Nir, and T. Volansky(2012), arXiv:1204.1975 [hep-ph]
- [52] L. M. Carpenter, A. Rajaraman, and D. Whiteson(2010), arXiv:1010.1011 [hep-ph]
- [53] A. Lenz, U. Nierste, J. Charles, S. Descotes-Genon, A. Jantsch, *et al.*, Phys.Rev. **D83**, 036004 (2011), arXiv:1008.1593 [hep-ph]
- [54] A. Lenz, U. Nierste, J. Charles, S. Descotes-Genon, H. Lacker, *et al.*(2012), arXiv:1203.0238 [hep-ph]
- [55] A. Bevan *et al.* (UTfit Collaboration), PoS **ICHEP2010**, 270 (2010), arXiv:1010.5089 [hep-ph]
- [56] E. Lunghi and A. Soni, Phys.Lett. **B697**, 323 (2011), arXiv:1010.6069 [hep-ph]